JOC*Article*

Determination of the Absolute Configuration of a Chiral Oxadiazol-3-one Calcium Channel Blocker, Resolved Using Chiral Chromatography, via Concerted Density Functional Theory Calculations of Its Vibrational Circular Dichroism, Electronic Circular Dichroism, and Optical Rotation

P. J. Stephens* and F. J. Devlin

Department of Chemistry, University of Southern California, Los Angeles, California 90089-0482

F. Gasparrini and A. Ciogli

Dipartimento di Studi di Chimica e Tecnologia delle Sostanze Biologicamente Attive, Università degli Studi di Roma "La Sapienza", Piazzale A. Moro 5, Roma 00185, Italy

D. Spinelli

Dipartimento di Chimica Organica "A. Mangini", Università di Bologna, Via San Giacomo 11, Bologna 40126, Italy

B. Cosimelli

Dipartimento di Chimica Farmaceutica e Tossicologica, Università di Napoli "Federico II", Via Montesano 49, Napoli 80131, Italy

pstephen@usc.edu

Received February 14, 2007

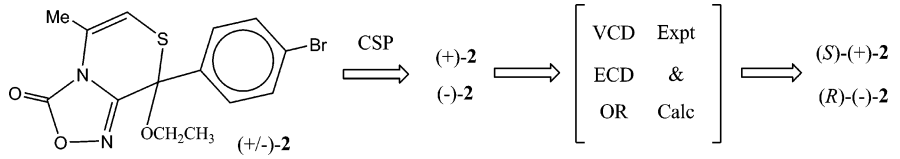

The chiral oxadiazol-3-one **2** has recently been shown to exhibit myocardial calcium entry channel blocking activity, substantially higher than that of diltiazem. To determine the enantioselectivity of this activity, the enantiomers of **2** have been resolved using chiral chromatography. The absolute configuration (AC) of **2** has been determined by comparison of density functional theory (DFT) calculations of its vibrational circular dichroism (VCD) spectrum, electronic circular dichroism (ECD) spectrum, and optical rotation (OR) to experimental VCD, ECD, and OR data. All three chiroptical properties yield identical ACs; the AC of **2** is unambiguously determined to be *S*(+)/*R*(−).

Introduction

As part of an ongoing search for new myocardial calcium channel modulators, a range of derivatives of the thiazino-oxadiazolone, **1**, were recently synthesized by Budriesi et al. and their activities as calcium entry channel blockers assayed.[1] The most active derivative found was 8-(4-bromophenyl)-8-ethoxy-5-methyl-8*H*-[1,4]thiazino-[3,4-*c*][1,2,4]oxadiazol-3-one, **2**. The activity of **2** was 20 times greater than that of diltiazem, a well-known and widely used L-type calcium entry blocker. The C8 carbon atom is stereogenic and **2** is a chiral molecule. In the study of Budriesi et al. racemic **2** was synthesized and assayed.[1] To determine the enantioselectivity of the calcium entry channel blocker activity of **2**, we have separated its two enantiomers, using chiral chromatography, and determined their individual activities. Since chromatography by itself does not define the absolute configurations (ACs) of the enantiomers of **2**, we have simultaneously determined their ACs

(1) Budriesi, R.; Carosati, E.; Chiarini, A.; Cosimelli, B.; Cruciani, G.; Ioan, P.; Spinelli, D.; Spisani, R. *J. Med. Chem.* **2005**, *48*, 2445−2456.

10.1021/jo070302k CCC: $37.00
Published on Web 05/22/2007

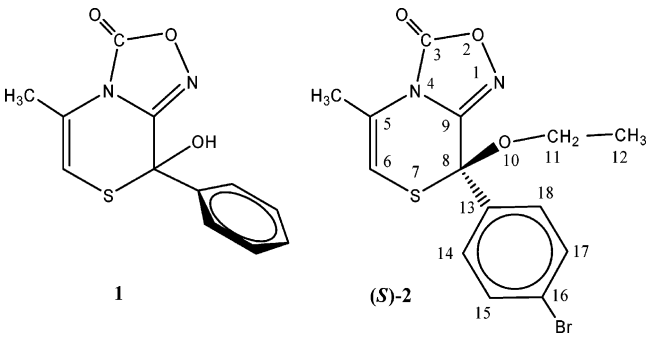

1 (*S*)-2

using chiroptical spectroscopies. Specifically, we have measured the vibrational circular dichroism (VCD), electronic circular dichroism (ECD), and optical rotatory dispersion (ORD) of **2** and used density functional theory (DFT) calculations of these chiroptical properties to elucidate their ACs. The application of DFT to the calculation of VCD spectra, using Stephens' equation for vibrational rotational strengths,[2] began in the early 1990s[3] and culminated in the full DFT implementation of Cheeseman et al.[3f] in 1996, subsequently incorporated in the widely distributed program GAUSSIAN.[4] The application of time-dependent DFT (TDDFT) to the calculation of optical rotation[5] and ECD spectra[6] followed soon thereafter. The development of the DFT methods for calculating VCD, OR, and ECD has revolutionized the determination of ACs using these chiroptical properties and their use is rapidly increasing.[5−7] While ACs can be determined by using only a single chiroptical property, the concerted use of all three properties clearly provides more definitive ACs. Examples of the power of concerted DFT calculations of VCD, ECD, and OR in determining the ACs of natural products molecules are provided by recent studies of quadrone,[8] schizozygine,[9] and plumericin and iso plumericin.[10] In this paper, we report the concerted application of these three chiroptical techniques to the determination of the AC of **2**. Simultaneously, biological assays of the enantiomers of **2** have been carried out, establishing the enantioselectivity of its calcium entry channel blocking activity.[11]

Results

Chiral Chromatography. The enantiomers of **2** were well resolved by enantioselective HPLC on the (*R,R*)-DACH-DNB chiral stationary phase under normal phase conditions with both UV and CD detection ($k_1 = 3.98$; $\alpha = 1.14$; $T = 25$ °C) (Figure 1a). Scaling-up to semipreparative conditions was straightforward, and 15 replicate separations (2.7 mg of sample each run) carried out on a 1.0 cm internal diameter (*R,R)*-DACH-DNB column afforded the two enantiomers with ee values greater than 96% and overall recovery of ∼65%. In particular, we obtained 12 mg of (−)-**2** and 14 mg of (+)-**2** from about 40 mg of (±)-**2**. By using analytical HPLC, UV and ECD at 270 nm were recorded for each stereoisomer; the ee values of the first eluted enantiomer (Figure 1b) and the second eluted enantiomer (Figure 1c) were determined to be 99% and 96%, respectively.

ECD. The UV and ECD spectra of (+)-**2** and (−)-**2** were measured using 4.1×10^{-5} M solutions in CH_3CN with the results shown in Figure 2.

Experimental IR and VCD Spectra. The IR and VCD spectra of (+)-**2**, (−)-**2**, and (±)-**2** were measured using solutions in $CDCl_3$. Concentrations were 0.04−0.05 M and the cell pathlength was 597 μm. After subtraction of the VCD spectrum of (±)-**2**, the VCD spectra of (+)-**2** and (−)-**2** were normalized to 100% ee, with the results given in Figure 3a. The VCD spectra of the two enantiomers are close to mirror images of each other, as further demonstrated in Figure 3b, where the "half-difference" and "half-sum" spectra, $^1/_2[\Delta\epsilon(+) - \Delta\epsilon(-)]$ and $^1/_2[\Delta\epsilon(+) + \Delta\epsilon(-)]$, are displayed. If the VCD spectra of the two enantiomers are exact mirror images, $\Delta\epsilon(+) = -\Delta\epsilon(-)$, the "half-sum" spectrum is exactly zero, and the "half-difference" spectrum is equal to $\Delta\epsilon(+)$. The deviations from zero observed in the experimental "half-sum" spectrum

(2) Stephens, P. J. *J. Phys. Chem.* **1985**, *89*, 748−752.
(3) (a) Stephens, P. J.; Devlin, F. J.; Chabalowski, C. F.; Frisch, M. J. *J. Phys. Chem.* **1994**, *98*, 11623−11627. (b) Stephens, P. J.; Devlin, F. J.; Ashvar, C. S.; Chabalowski, C. F.; Frisch, M. J. *Faraday Discuss.* **1994**, *99*, 103−119. (c) Bak, K. L.; Devlin, F. J.; Ashvar, C. S.; Taylor, P. R.; Frisch, M. J.; Stephens, P. J. *J. Phys. Chem.* **1995**, *99*, 14918−14922. (d) Devlin, F. J.; Finley, J. W.; Stephens, P. J.; Frisch, M. J. *J. Phys. Chem.* **1995**, *99*, 16883−16902. (e) Stephens, P. J.; Devlin, F. J.; Ashvar, C. S.; Bak, K. L.; Taylor, P. R.; Frisch, M. J. In *Chemical Applications of Density−Functional Theory*; ACS Symp. Ser.; Laird, B. B., Ross, R. B., Ziegler, T., Eds.; American Chemical Society: Washington, DC, 1996; Vol. 629, pp 105−113. (f) Cheeseman, J. R.; Frisch, M. J.; Devlin, F. J.; Stephens, P. J. *Chem. Phys. Lett.* **1996**, *252*, 211−220.
(4) GAUSSIAN, Gaussian Inc.: www.gaussian.com.
(5) (a) Stephens, P. J.; Devlin, F. J.; Cheeseman, J. R.; Frisch, M. J.; Mennucci, B.; Tomasi, J. *Tetrahedron*: *Asymmetry* **2000**, *11*, 2443−2448. (b) Stephens, P. J.; Devlin, F. J.; Cheeseman, J. R.; Frisch, M. J. *J. Phys. Chem. A* **2001**, *105*, 5356−5371. (c) Stephens, P. J.; Devlin, F. J.; Cheeseman, J. R.; Frisch, M. J. *Chirality* **2002**, *14*, 288−296. (d) Stephens, P. J.; Devlin, F. J.; Cheeseman, J. R.; Frisch, M. J.; Rosini, C. *Org. Lett.* **2002**, *4*, 4595−4598. (e) Stephens, P. J.; Devlin, F. J.; Cheeseman, J. R.; Frisch, M. J.; Bortolini, O.; Besse, P. *Chirality* **2003**, *15*, S57−S64. (f) McCann, D. M.; Stephens, P. J.; Cheeseman, J. R. *J. Org. Chem.* **2004**, *69*, 8709−8717.
(6) (a) Stephens, P. J.; McCann, D. M.; Butkus, E.; Stoncius, S.; Cheeseman, J. R.; Frisch, M. J. *J. Org. Chem.* **2004**, *69*, 1948−1958. (b) Stephens, P. J.; McCann, D. M.; Devlin, F. J.; Cheeseman, J. R.; Frisch, M. J. *J. Am. Chem. Soc.* **2004**, *126*, 7514−7521. (c) McCann, D. M.; Stephens, P. J. *J. Org. Chem.* **2006**, *71*, 6074−6098.
(7) See, for example: (a) Ashvar, C. S.; Stephens, P. J.; Eggimann, T.; Wieser, H. *Tetrahedron*: *Asymmetry* **1998**, *9*, 1107−1110. (b) Aamouche, A.; Devlin, F. J.; Stephens, P. J. *Chem. Commun.* **1999**, 361−362. (c) Stephens, P. J.; Devlin, F. J. *Chirality* **2000**, *12*, 172−179. (d) Aamouche, A.; Devlin, F. J.; Stephens, P. J. *J. Am. Chem. Soc.* **2000**, *122*, 2346−2354. (e) Aamouche, A.; Devlin, F. J.; Stephens, P. J.; Drabowicz, J.; Bujnicki, B.; Mikolajczyk, M. *Chem. Eur. J.* **2000**, *6*, 4479−4486. (f) Stephens, P. J.; Aamouche, A.; Devlin, F. J.; Superchi, S.; Donnoli, M. I.; Rosini, C. *J. Org. Chem.* **2001**, *66*, 3671−3677. (g) Devlin, F. J.; Stephens, P. J.; Scafato, P.; Superchi, S.; Rosini, C. *Tetrahedron*: *Asymmetry* **2001**, *12*, 1551−1558. (h) Stephens, P. J.; Devlin, F. J.; Aamouche, A. In *Chirality*: *Physical Chemistry*; ACS Symp. Ser.; Hicks, J. M., Ed.; American Chemical Society: Washington, DC, 2002; Vol. 810, Chapter 2, pp 18−33. (i) Devlin, F. J.; Stephens, P. J.; Scafato, P.; Superchi, S.; Rosini, C. *Chirality* **2002**, *14*, 400−406. (j) Devlin, F. J.; Stephens, P. J.; Oesterle, C.; Wiberg, K. B.; Cheeseman, J. R.; Frisch, M. J. *J. Org. Chem.* **2002**, *67*, 8090−8096. (k) Stephens, P. J. In *Computational Medicinal Chemistry for Drug Discovery*; Bultinck, P., de Winter, H., Langenaecker, W., Tollenaere, J., Eds.; Dekker: New York, 2003, Chapter 26, pp 699−725. (l) Cere, V.; Peri, F.; Pollicino, S.; Ricci, A.; Devlin, F. J.; Stephens, P. J.; Gasparrini, F.; Rompietti, R.; Villani, C. *J. Org. Chem.* **2005**, *70*, 664−669. (m) Stephens, P. J.; McCann, D. M.; Devlin, F. J.; Flood, T. C.; Butkus, E.; Stoncius, S.; Cheeseman, J. R. *J. Org. Chem.* **2005**, *70*, 3903−3913. (n) Devlin, F. J.; Stephens, P. J.; Besse, P. *Tetrahedron*: *Asymmetry* **2005**, *16*, 1557−1566. (o) Devlin, F. J.; Stephens, P. J.; Bortolini, O. *Tetrahedron*: *Asymmetry* **2005**, *16*, 2653−2663.
(8) Stephens, P. J.; McCann, D. M.; Devlin, F. J.; Smith, A. B., III *J. Nat. Prod.* **2006**, *69*, 1055−1064.
(9) Stephens, P. J.; Pan, J. J.; Devlin, F. J.; Urbanová, M.; Hájíček J. *J. Org. Chem.* **2007**, *72*, 2508−2524.
(10) Stephens, P. J.; Pan, J. J.; Devlin, F. J.; Krohn, K.; Kurtán, T. *J. Org. Chem.* **2007**, *72*, 3521−3536.
(11) Carosati, E.; Cruciani, G.; Chiarini, A.; Budriesi, R.; Ioan, P.; Spisani, R.; Spinelli, D.; Cosimelli, B.; Fusi, F.; Frosini, M.; Matucci, R.; Gasparrini, F.; Ciogli, A.; Stephens, P. J.; Devlin, F. J. *J. Med. Chem.* **2006**, *49*, 5206−5216.

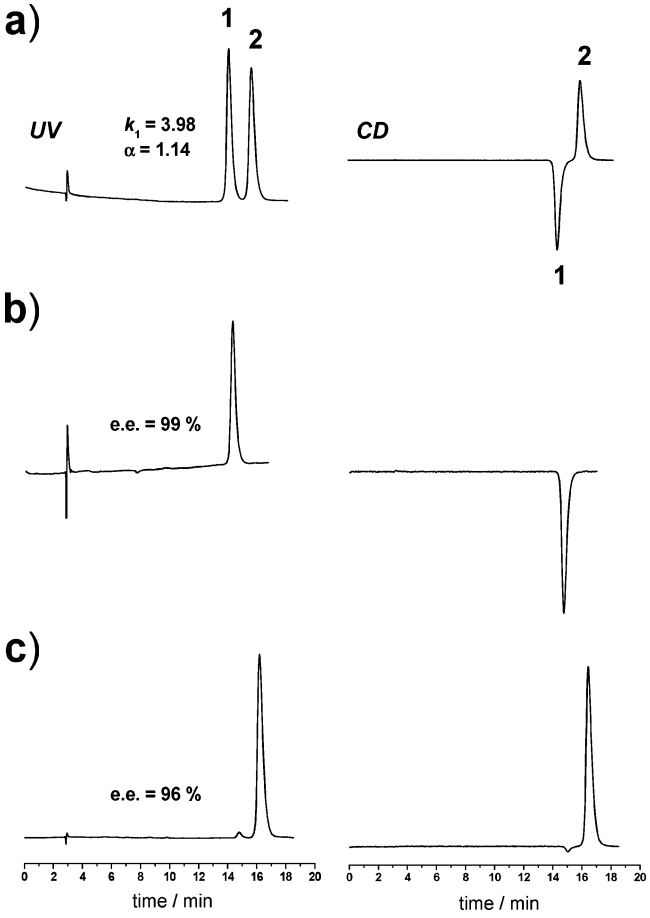

FIGURE 1. Analytical separation of the enantiomers of **2** by enantioselective HPLC [column, (*R*,*R*)-DACH-DNB 5 μ (250 mm × 4.6 mm i.d.); eluent, *n*-hexane/dichloromethane 70/30, v/v; flow rate, 1.0 mL/min at 25 °C; UV (left) and CD (right) at 270 nm]: (**a**) racemic mixture; (**b** and **c**) peak purity checks of the pooled fractions containing (−)-**2** (ee 99%) and (+)-**2** (ee 96%) enantiomers, respectively, after semipreparative enantioselective HPLC.

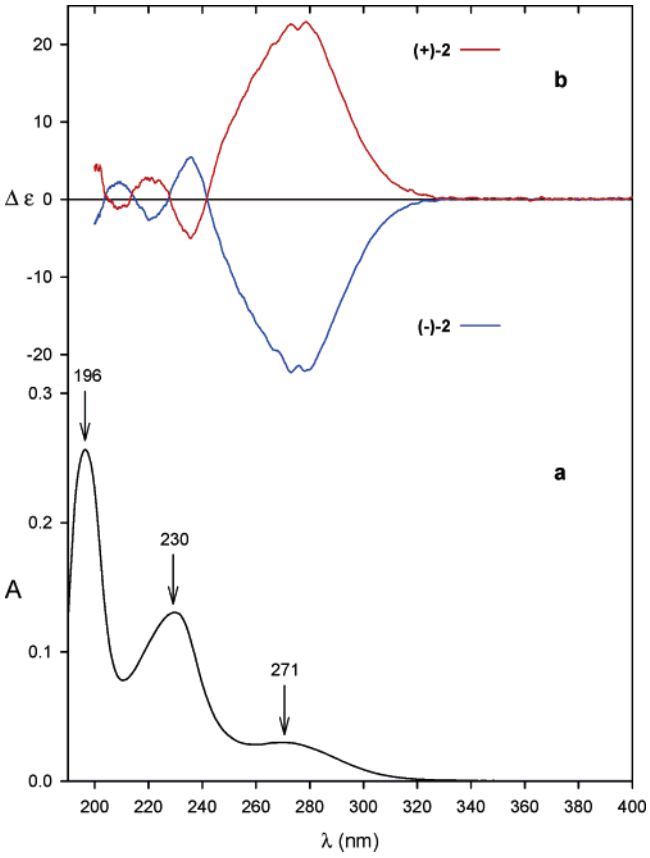

FIGURE 2. UV (**a**), and CD (**b**) spectra of 4.1 × 10^{-5} M CH_3CN solutions of (+)-**2** and (−)-**2**.

reflect both non-reproducible noise and artifact signals. As can be seen in Figure 3b, the deviation from zero of the "half-sum" spectrum is overall very small compared to the "half-difference" spectrum, demonstrating that the latter is a good approximation to the exact VCD of (+)-**2**. The "half-difference" spectrum, $\Delta\epsilon(+)$, is compared to the IR spectrum of (±)-**2** in Figure 4.

Conformational Analysis. Molecule **2** is conformationally flexible: the 6-membered thiazino ring is anticipated to be nonplanar, and therefore to have two or more conformations; the phenyl ring can rotate around the C8−C13 bond; and the ethoxy group can rotate around the C8−O10 and O10−C11 bonds. The measurements of the VCD, ECD, and OR of **2** are carried out at room temperature, and calculation of the structures, relative free energies and percentage populations of the stable conformations of **2** which are populated at room temperature is therefore prerequisite to the calculation of the VCD, ECD, and OR of **2**.

As in prior studies of highly flexible molecules in our laboratories,[5f,6a−c,7l−o,8−10] conformational analysis is initially carried out using molecular mechanics, specifically using the MMFF94 force field together with the conformational searching procedures of SPARTAN 02.[12] With a window of 10 kcal/mol, 16 MMFF94 conformers were found, with the relative energies given in Table 1. Reoptimization with DFT at the B3LYP/6-31G* level led to 13 independent conformers, with the relative energies given in Table 2. Calculations of harmonic vibrational frequencies for all 13 conformations confirmed their stability and led to the relative free energies given in Table 2. These in turn allow the room temperature equilibrium populations to be calculated, with the results also given in Table 2. Only three conformations, labeled **a**, **b**, and **c**, have free energies with <2 kcal/mol and populations >2 %. Further optimizations of these three conformations, followed by vibrational frequency and free energy calculations, were then carried out using the two functionals B3LYP and B3PW91, together with the basis set TZ2P,[3,7] which is substantially larger and more accurate than 6-31G*, with the results also given in Table 2.

The structures of conformations **a**, **b**, and **c** at the B3LYP/6-31G* level are shown in Figure 5. Key dihedral angles of the B3LYP/6-31G*, B3LYP/TZ2P, and B3PW91/TZ2P geometries of conformations **a**, **b**, and **c** are given in Table 3 and show that the structures are insensitive to both functional and basis set. In each conformation, the oxadiazolone ring is very close to planar and the thiazino ring is similarly puckered. On the other hand, the conformations of the ethyl group are different in **a**, **b**, and **c**. The B3LYP/6-31G* dihedral angle C9C8O10C11 is 170.2°, −58.3°, and 59.3° and the dihedral angle C8O10C11C12 is 170.1°, −173.5°, and −177.7° in **a**, **b**, and **c** respectively. Thus, the three expected staggered conformations of the CH_2 group relative to the thiazino ring are found, while in each rotamer, the CH_3 group is trans to C8. The conformations of

(12) Spartan 02; Wavefunction, Inc.: www.wavefun.com.

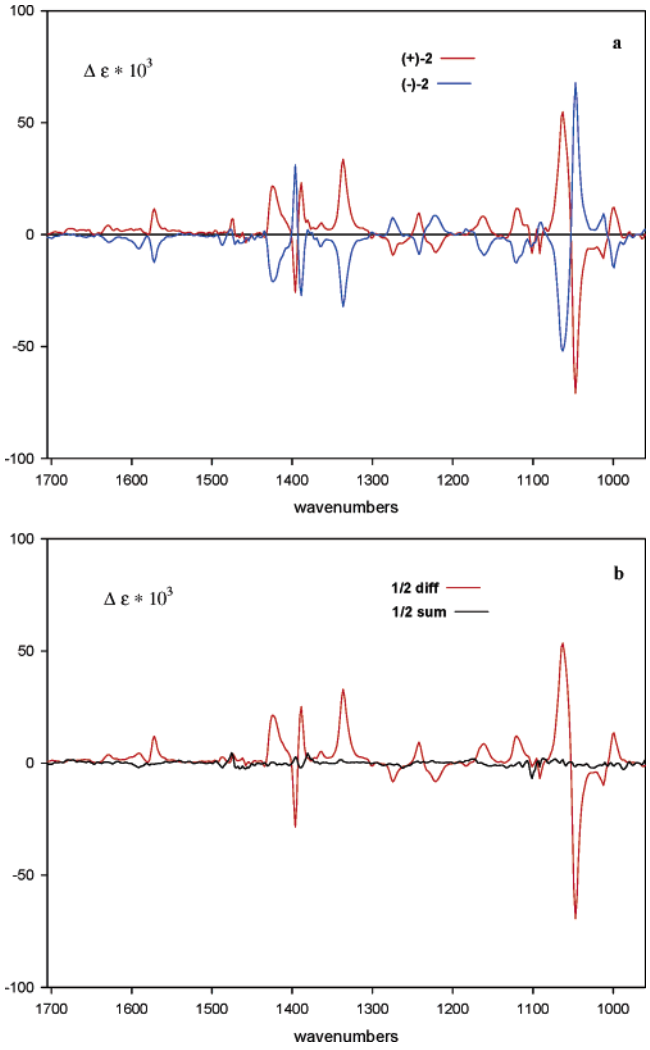

FIGURE 3. (**a**) Mid-IR VCD spectra of (+)-**2** and (−)-**2**, normalized to 100% ee; (**b**) half-difference and half-sum VCD spectra.

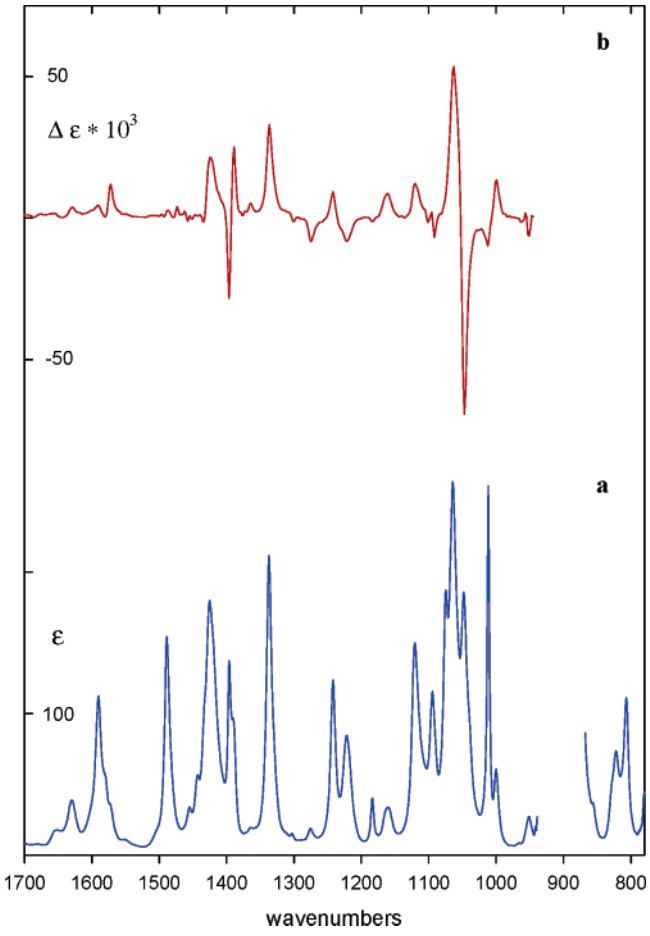

FIGURE 4. (**a**) IR spectrum of (±)-**2**; (**b**) VCD spectrum of (+)-**2**. The gap at ∼900 cm^{-1} is due to strong absorption of the $CDCl_3$ solvent.

TABLE 1. MMFF94 Conformations of 2

conformer	ΔE^a	B3LYP/6-31G* conformation[b]
1	0.00	**b**
2	1.97	**b**
3	3.12	**e**
4	3.13	**g**
5	3.14	**a**
6	3.33	**g**
7	3.51	**c**
8	3.81	**j**
9	4.58	**h**
10	7.22	**m**
11	7.23	**l**
12	7.24	**f**
13	7.31	**d**
14	7.58	**i**
15	8.59	**h**
16	8.70	**k**

[a] ΔE in kcal/mol. [b] See Table 2.

the *p*-Br-phenyl group vary somewhat in **a**−**c**, undoubtedly reflecting the varying steric interaction with the ethyl group.

To further refine our understanding of the conformations of **2**, we have carried out two B3LYP/6-31G* scans of its PES, starting from conformation **a** and varying separately the two dihedral angles N4C9C8S7 and C9C8C13C14, with the results given in Figures 6 and 7. The second, oppositely puckered, conformation of the thiazino ring is found to lie >3 kcal/mol higher in energy than the conformation occurring in **a**−**c**. As expected, no additional rotamers of the *p*-Br-phenyl group are found.

Calculation of IR and VCD Spectra. The harmonic vibrational frequencies, dipole strengths, and rotational strengths of conformations **a**−**c** have been calculated using DFT at the B3LYP/TZ2P and B3PW91/TZ2P levels, via GAUSSIAN 03, with the results given in Table 2 of the Supporting Information. The IR and VCD spectra of the three conformations are obtained thence, assuming Lorentzian bandshapes, with the results shown in Figures 1 and 2 of the Supporting Information. As expected, on the basis of prior studies of conformationally flexible molecules,[7] both IR and VCD spectra of the three conformations vary substantially, the variation being greater for the VCD spectra. The spectra of the three conformations, weighted by their room temperature equilibrium populations, are shown in Figures 8 and 9. The conformationally averaged spectra (i.e., the sum of the population-weighted spectra of the three conformations) are shown in Figures 10 and 11, together with the experimental spectra. The conformationally averaged spectra are dominated by the contributions of conformer **a**. The contributions of conformer **b** are resolved here and there, but are mostly submerged under the contributions of **a**. The contributions of conformer **c** are so weak that they are not detectable in the conformationally averaged spectra. Comparison

TABLE 2. DFT Relative Energies, Relative Free Energies, and Populations of the Conformations of 2

conformer[c]	B3LYP/6-31G*			B3LYP/TZ2P			B3PW91/TZ2P		
	ΔE^a	ΔG^a	P (%)[b]	ΔE^a	ΔG^a	P (%)[b]	ΔE^a	ΔG^a	P (%)[b]
a	0.00	0.00	54.6	0.00	0.00	80.7	0.00	0.00	84.8
b	0.26	0.22	37.7	0.78	0.93	16.8	0.95	1.11	13.0
c	1.68	1.74	2.9	1.90	2.05	2.5	1.91	2.16	2.2
d	2.40	2.01	1.8						
e	2.36	2.28	1.2						
f	2.56	2.33	1.1						
g	3.24	3.04	0.3						
h	3.07	3.07	0.3						
i	3.22	3.69	0.1						
j	2.88	3.94	0.1						
k	6.19	6.52	0.0						
l	6.32	6.55	0.0						
m	7.37	7.38	0.0						

[a] ΔE and ΔG in kcal/mol. [b] Populations based on ΔG values, T = 298 K. [c] Key dihedral angles of the B3LYP/6-31G* conformations of (*S*)-**2** are given in Table 1 of the Supporting Information.

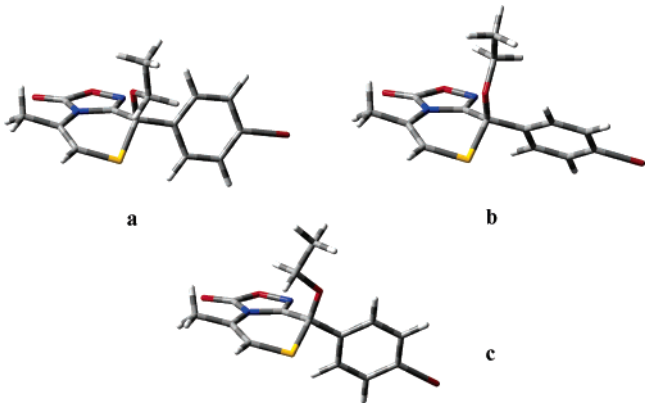

FIGURE 5. B3LYP/6-31G* structures of conformations **a**, **b**, and **c** of (*S*)-**2**.

of the B3LYP/TZ2P and B3PW91/TZ2P IR spectra to the experimental IR spectrum (Figure 10) shows that the B3PW91 spectrum is in excellent agreement with experiment, and that the B3LYP spectrum is in not-so-good agreement. Accordingly, we assign the experimental spectrum on the basis of the

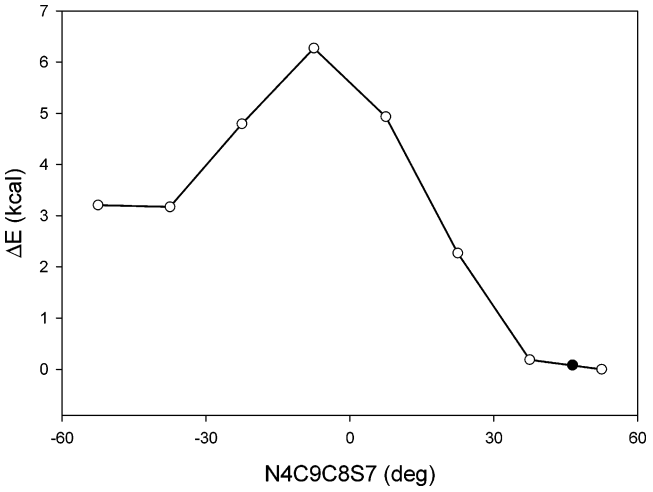

FIGURE 6. B3LYP/6-31G* PES scan with respect to the thiazino ring dihedral N4C9C8S7 of (*S*)-**2**: ●, dihedral angle of **2a**.

B3PW91/TZ2P calculated spectrum, as detailed in Table 2 of the Supporting Information and Figure 10. Using this assignment, experimental values for the frequencies and dipole strengths are extracted from the experimental IR spectrum via Lorentzian fitting, as we have carried out in prior publications,[3,7,13] with the results given in Table 2 of the Supporting Information. Comparison of calculated and experimental frequencies and dipole strengths is shown in Figure 3 of the Supporting Information and in Figure 12. The systematic overestimation of frequencies is predominantly due to the neglect of anharmonicity in the calculations.[14] The agreement of calculated and experimental dipole strengths is good, providing strong support for the assignment of the IR spectrum.

Comparison of the B3LYP/TZ2P and B3PW91/TZ2P VCD spectra of *S*-**2** to the experimental spectrum of (+)-**2** (Figure 11), as with the IR spectra, shows that the B3PW91 spectrum is in better, and excellent, agreement with experiment. Again, the assignment of the experimental VCD spectrum is therefore based on the B3PW91/TZ2P calculated spectrum, together with the assignment of the experimental IR spectrum,

TABLE 3. Dihedral Angles[a] of the Conformations a−c of (*S*)-2

dihedral angle	B3LYP/6-31G*			B3LYP/TZ2P			B3PW91/TZ2P		
	a	**b**	**c**	**a**	**b**	**c**	**a**	**b**	**c**
N4C3O2N1	0.3	0.1	0.6	0.5	0.4	0.7	0.4	0.2	0.6
C3O2N1C9	0.2	0.8	−0.1	0.0	0.5	−0.4	0.1	0.6	−0.3
O2N1C9N4	−0.7	−1.5	−0.4	−0.5	−1.1	−0.1	−0.5	−1.2	0.0
N1C9N4C3	0.9	1.6	0.8	0.8	1.4	0.5	0.8	1.3	0.4
C9N4C3O2	−0.7	−0.9	−0.8	−0.7	−1.0	−0.7	−0.7	−0.9	−0.6
N4C9C8S7	46.4	44.9	34.3	46.2	44.7	33.4	46.6	45.2	33.7
C9C8S7C6	−50.1	−48.5	−37.5	−49.8	−48.3	−36.7	−50.3	−48.9	−37.1
C8S7C6C5	32.7	31.2	26.2	32.5	31.2	25.6	32.9	31.6	26.0
S7C6C5N4	0.0	0.1	−1.9	0.2	0.3	−1.4	0.1	0.3	−1.5
C6C5N4C9	−18.5	−17.0	−12.7	−18.4	−17.3	−13.2	−18.5	−17.4	−13.2
C5N4C9C8	−10.3	−10.5	−7.9	−10.4	−10.4	−7.2	−10.4	−10.4	−7.2
C9C8O10C11	170.2	−58.3	59.3	170.0	−57.1	59.3	170.6	−57.5	60.1
S7C8O10C11	57.2	−172.4	−61.9	57.0	−171.1	−61.8	57.4	−171.6	−61.2
C13C8O10C11	−68.3	71.9	−178.0	−68.1	73.3	−177.9	−67.6	72.9	−177.2
C8O10C11C12	170.1	−173.5	−177.7	171.8	−172.8	−177.9	173.1	−172.9	−178.2
O10C8C13C14	155.4	24.7	7.4	155.2	21.9	4.1	154.2	21.9	3.3
C9C8C13C14	−87.7	151.7	130.0	−87.3	149.3	126.9	−88.1	149.5	126.3
S7C8C13C14	28.9	−91.1	−113.5	28.8	−94.1	−116.8	27.7	−94.3	−117.7

[a] Dihedral angles are in degrees.

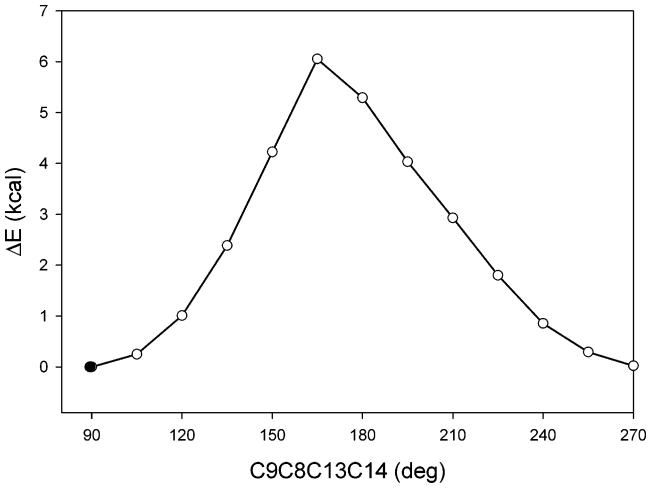

FIGURE 7. B3LYP/6-31G* PES scan with respect to the phenyl group dihedral angle C9C8C13C14 of (*S*)-**2**: ●, dihedral angle of **2a**.

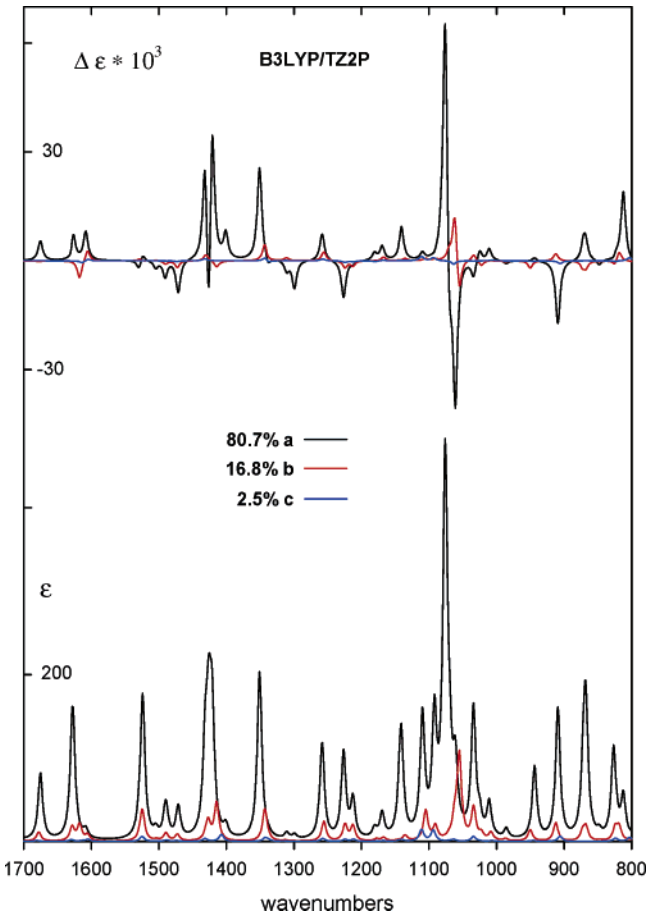

FIGURE 8. Equilibrium population weighted B3LYP/TZ2P IR and VCD spectra of conformations **a**−**c** of (*S*)-**2**. Lorentzian bandwidths $\gamma = 4.0$ cm^{-1}.

since the assignments of the two spectra must of course be consistent. The assignment arrived at is detailed in Table 2 of the Supporting Information and Figure 11. On the basis of this assignment, experimental frequencies and rotational strengths are extracted from the experimental VCD spectrum, via Lorentzian fitting, with the results given in Table 2 of the Supporting Information. Calculated and experimental rotational strengths are compared in Figure 13. The agreement is exceptionally good,

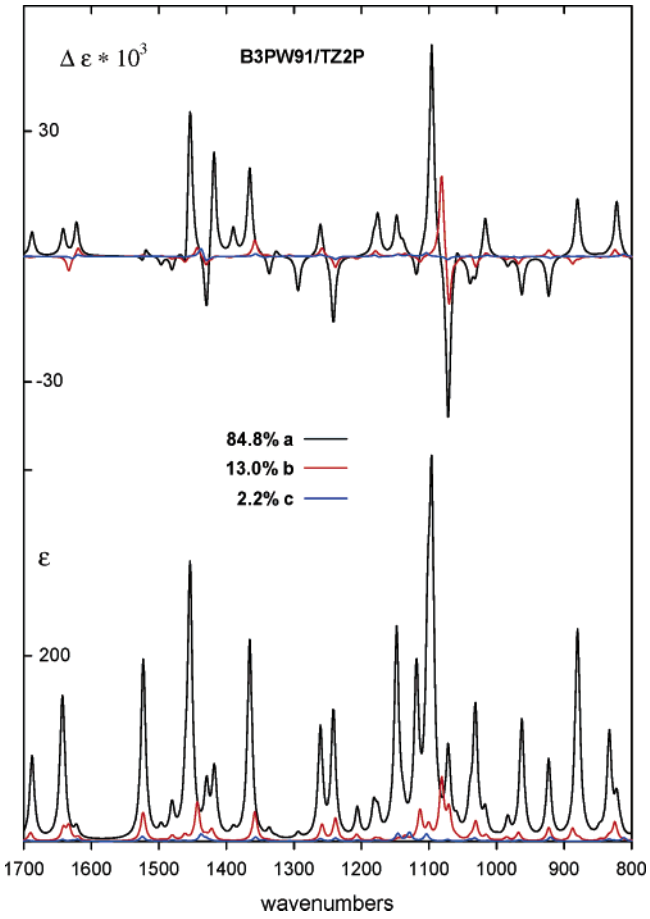

FIGURE 9. Equilibrium population weighted B3PW91/TZ2P IR and VCD spectra of conformations **a**−**c** of (*S*)-**2**. Lorentzian bandwidths $\gamma = 4.0$ cm^{-1}.

leading unambiguously to the conclusion that the AC of (+)-**2** is *S*. Comparison of the calculated rotational strengths for *R*-**2** to the experimental values for (+)-**2** shows that agreement is so bad (Figure 13) that there is no possibility that the AC is *R*-(+).

Optical Rotations. The specific rotations of (−)-**2** in $CDCl_3$ solution have been measured at the sodium D line and at 578, 546, and 436 nm, with the results given in Table 4. The specific rotations at these four wavelengths have been calculated using TDDFT at the B3LYP/aug-cc-pVDZ//B3LYP/6-31G* and B3PW91/aug-cc-pVDZ//B3LYP/6-31G* levels for conformations **a**−**c** with the results for *R*-**2** given in Table 4. The conformationally averaged rotations are also given in Table 4 and are compared to the experimental rotations of (−)-**2** in Figure 14. The B3LYP and B3PW91 functionals give very similar results. For both B3LYP and B3PW91 functionals, the agreement of calculated and experimental rotations is excellent for *R*-**2** and very bad for *S*-**2**, leading unambiguously to the conclusion that the AC is *S*-(+)/*R*-(−), the identical AC to that arrived at from the VCD spectrum.

(13) (a) Kawiecki, R. W.; Devlin, F. J.; Stephens, P. J.; Amos, R. D.; Handy, N. C. *Chem. Phys. Lett.* **1988**, *145*, 411−417. (b) Devlin, F. J.; Stephens, P. J.; Cheeseman, J. R.; Frisch, M. J. *J. Phys. Chem. A* **1997**, *101*, 6322−6333. (c) Devlin, F. J.; Stephens, P. J.; Cheeseman, J. R.; Frisch, M. J. *J. Phys. Chem. A* **1997**, *101*, 9912−9924.

(14) Finley, J. W.; Stephens, P. J. *J. Mol. Struct.* (*THEOCHEM*) **1995**, *357*, 225−235.

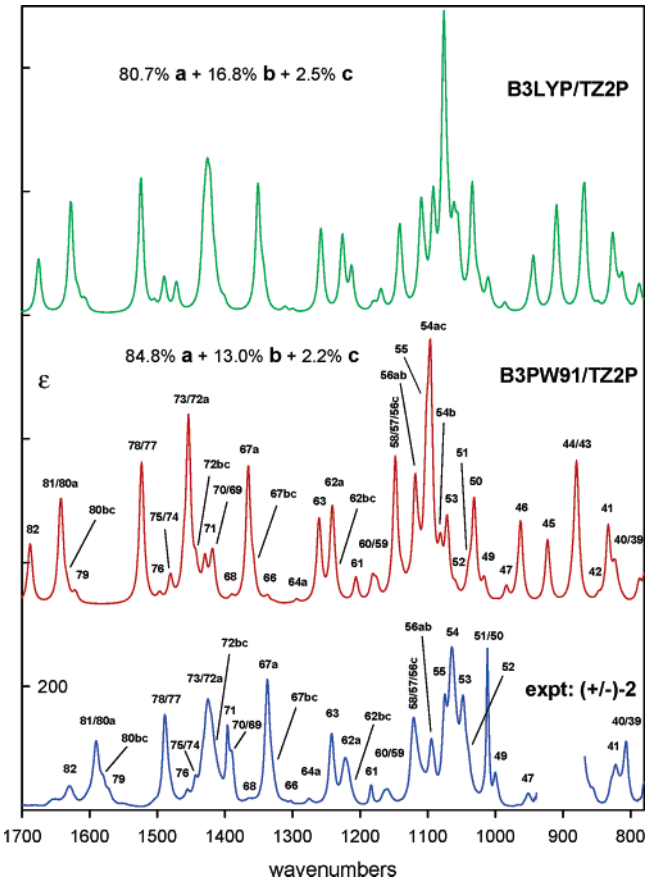

FIGURE 10. Comparison of the conformationally averaged B3LYP/TZ2P and B3PW91/TZ2P IR spectra of **2** to the experimental IR spectrum of (±)-**2**. Assignment of the latter is based on the B3PW91/TZ2P spectrum (see also Table 2 in the Supporting Information). The numbers are those of the fundamentals. When no conformation is specified the fundamentals of **a**, **b**, and **c** are unresolved.

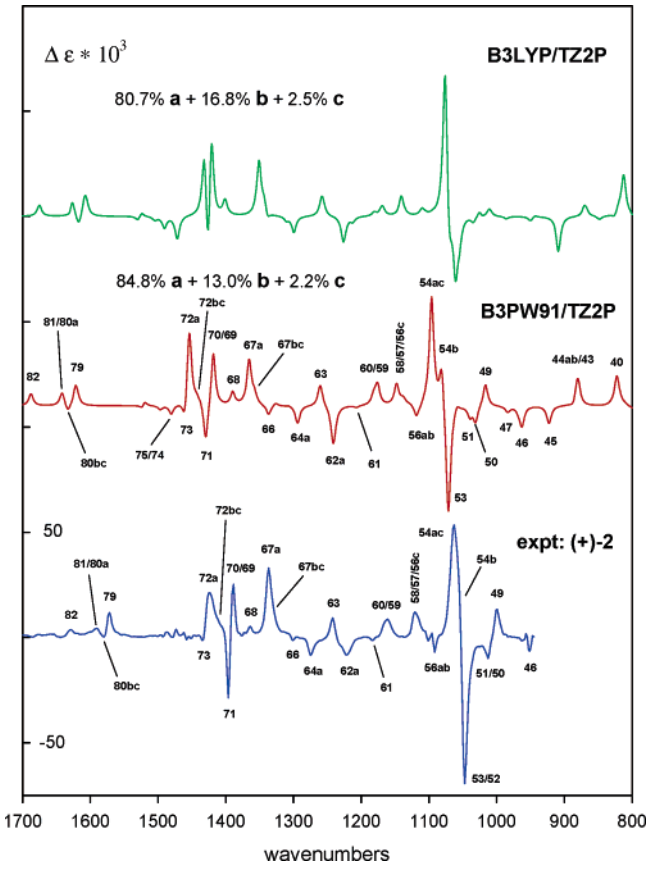

FIGURE 11. Comparison of the conformationally averaged B3LYP/TZ2P and B3PW91/TZ2P VCD spectra of (*S*)-**2** to the experimental VCD spectrum of (+)-**2**. Assignment of the latter is based on the assignment of the IR spectrum (Figure 10) and on the B3PW91/TZ2P VCD spectrum. The numbers are those of the fundamentals. When no conformation is specified the fundamentals of **a**, **b**, and **c** are unresolved.

Calculations of the Electronic Circular Dichroism (ECD). The excitation energies, oscillator strengths, and rotational strengths of the 15 lowest energy electronic excitations of conformations **a**−**c** of *S*-**2** have been calculated by using TDDFT at the B3LYP/aug-cc-pVDZ//B3LYP/6-31G* and B3PW91/aug-cc-pVDZ//B3LYP/6-31G* levels with the results given in Table 3 of the Supporting Information. Rotational strengths were calculated by using both length and velocity representations. The differences between length and velocity rotational strengths are very small, confirming that the aug-cc-pVDZ basis set is close to the complete basis set limit. The origin-independent velocity rotational strengths, weighted by the conformational populations given in Table 2, are plotted in Figure 15, together with the conformationally averaged ECD spectra, obtained by using Gaussian bandshapes[6c] with bandwidth parameters $\sigma = 0.2$ and 0.4 eV. Both B3LYP and B3PW91 functionals give very similar ECD spectra. In both cases, the ECD spectrum exhibits an intense band at ∼300 nm, of positive sign for *S*-**2**, and weaker bands of oscillating sign at higher energies. The qualitative agreement with the experimental ECD of (+)-**2** is excellent, and very bad for (−)-**2**, unambiguously confirming that the AC of **2** is *S*(+)/*R*(−).

Discussion

In order to analyze the mechanism of the pharmaceutical activity of a chiral drug, its enantioselectivity must be determined. This requires the preparation of the individual enantiomers, the determination of their absolute configurations (ACs), and the measurement of their pharmaceutical activities. At this time, the resolution of the racemic compound using chiral

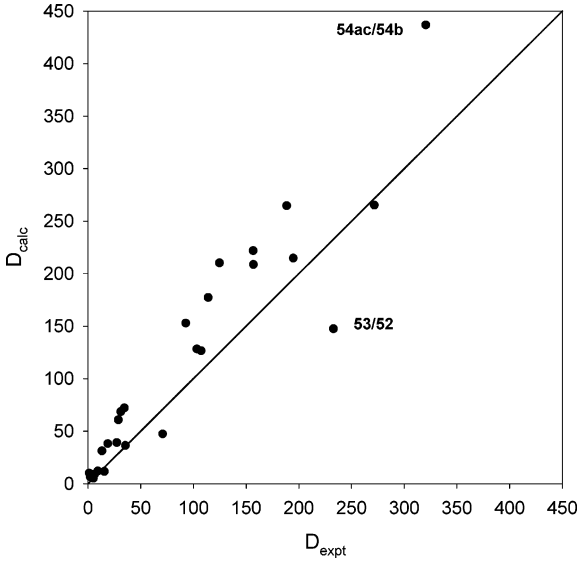

FIGURE 12. Comparison of B3PW91/TZ2P and experimental vibrational dipole strengths. Dipole strengths are in 10^{-40} esu^2 cm^2.

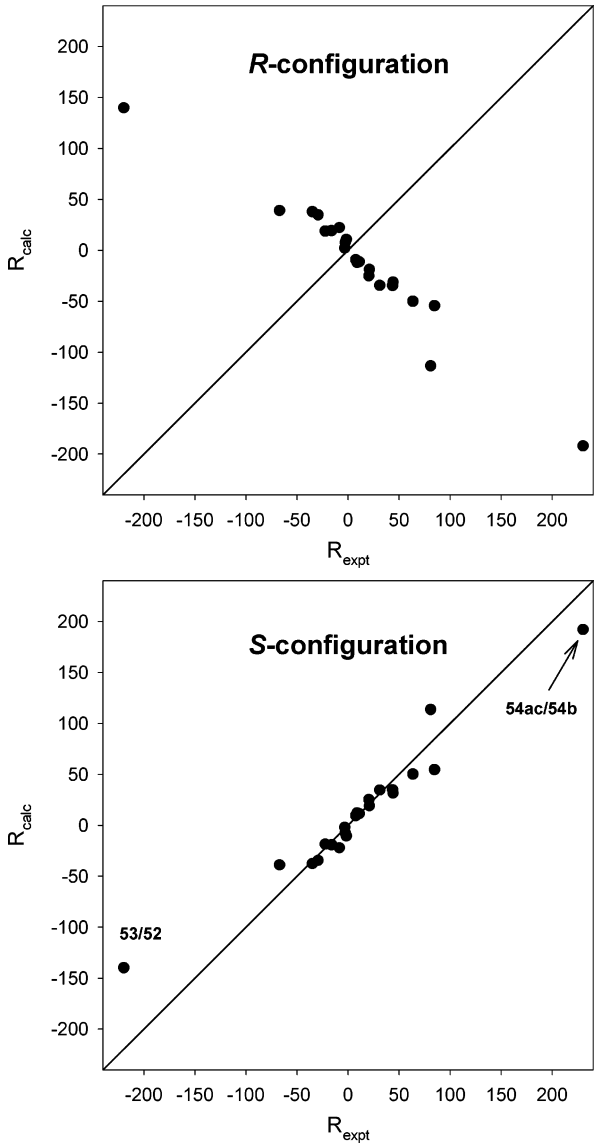

FIGURE 13. Comparison of B3W91/TZ2P rotational strengths for (*R*)-**2** and (*S*)-**2** to the experimental rotational strengths of (+)-**2**. Rotational strengths are in 10^{-44} esu^2 cm^2.

chromatography is the most efficient method for the preparation of the individual enantiomers. The concerted use of the chiroptical techniques, vibrational circular dichroism (VCD), electronic circular dichroism (ECD), and optical rotation (OR), is the most efficient method for the determination of the ACs of the enantiomers. To determine the ACs, DFT calculations of the VCD spectrum, the ECD spectrum, and the transparent spectral region ORD of the two enantiomers are compared to the experimental VCD, ECD, and ORD.

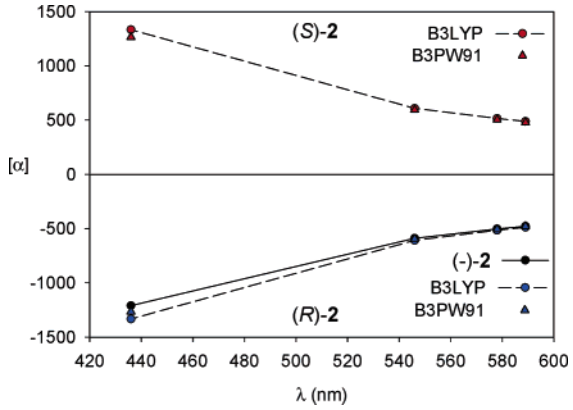

FIGURE 14. Comparison of the calculated specific rotations of (*R*)-**2** and (*S*)-**2** to the experimental rotations of (−)-**2**.

In this work, we illustrate the power of chiral chromatography combined with concerted chiroptical spectroscopy by determining the ACs of the enantiomers of the chiral oxadiazol-3-one, **2**. All three chiroptical techniques yield identical ACs: *S*(+)/*R*(−). Since it has been shown that the calcium entry channel blocking activity of (−)-**2** is greater than that of (+)-**2**,[11] it follows that the activity of *R*-**2** is greater than that of *S*-**2**.

Prior to the calculations of the VCD, ECD, and OR of **2**, conformational analysis of **2** is necessary. Using DFT we have shown that only three conformations of **2** are significantly populated at room temperature, these three conformations being rotamers of the ethoxy moiety. The excellent agreement of the predicted and experimental IR and VCD spectra of **2** strongly supports the reliability of the predicted structures and relative free energies of the conformations of **2**. We note also that the predicted conformation of the bicyclic thiazino-oxadiazolone moiety of **2**, which is the same in conformations **2a**, **2b**, and **2c**, is qualitatively identical to that of the X-ray structure of the *p*-chloro derivative of **1**.[15]

The calculations of the VCD, ECD, and ORD of **2** are carried out using state-of-the-art hybrid functionals and basis sets known to be good approximations to the complete basis set limit. Specifically, DFT VCD calculations use the functionals B3LYP and B3PW91 and the basis set TZ2P.[3,7] TDDFT ECD and OR calculations use the functionals B3LYP and B3PW91 and the basis set aug-cc-pVDZ.[5,6] As a result, the predicted VCD, ECD, and ORD are of high accuracy, and agreement of the calculated VCD, ECD, and ORD of *S*-and *R*-**2** with the experimental data for (+)- and (−)-**2** is excellent, leading unambiguously to the AC *S*(+)/*R*(−).

This work constitutes the first application of concerted DFT calculations of VCD, ECD, and ORD to the determination of the AC of a synthetic chiral compound exhibiting pharmaceutical activity. Prior applications to natural products with pharmaceuti-

TABLE 4. Calculated and Experimental Specific Rotations of 2

		[α]^b (calcd)							
		B3LYP				B3PW91			
λ (nm)	[α]^a (exptl)	**a**	**b**	**c**	CA^c	**a**	**b**	**c**	CA^c
589	−477.9	−790.0	−133.1	−238.0	−488.4	−779.3	−122.8	−231.0	−478.5
578	−502.9	−832.5	−142.9	−252.9	−515.8	−821.0	−131.9	−245.3	−505.1
546	−589.5	−975.5	−177.7	−304.5	−608.4	−961.2	−164.1	−295.0	−595.2
436	−1209.6	−2001.8	−580.7	−732.0	−1333.1	−1961.8	−461.9	−704.4	−1265.7

^{a} (−)-**2** in $CDCl_3$ ($c = 0.88$). ^{b} [α] for *R*-**2** calculated at the B3LYP/6-31G* geometry, using both the B3LYP and B3PW91 functionals and the aug-cc-pVDZ basis set. ^{c} Conformational average, obtained from populations based on ΔG values given in Table 2.

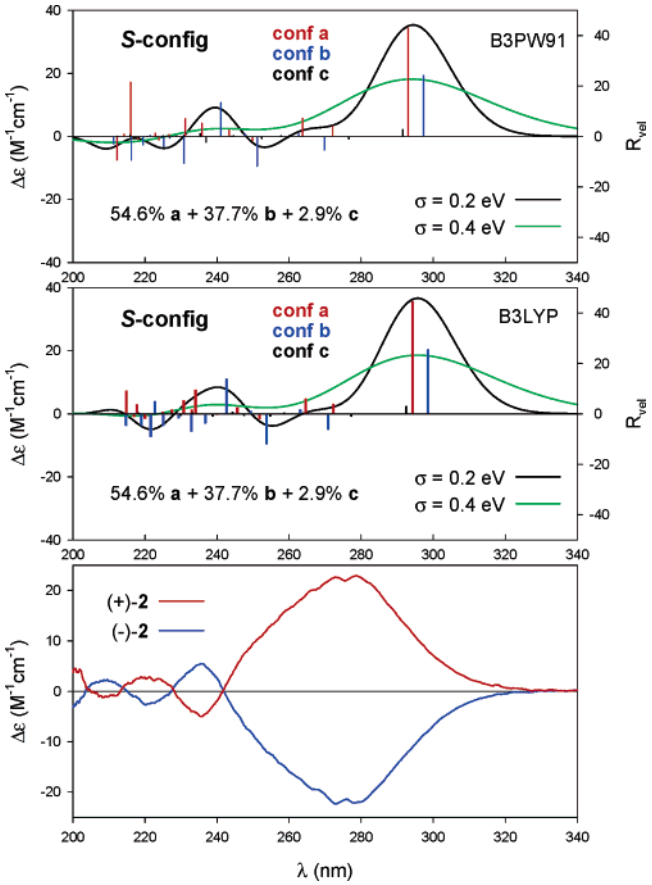

FIGURE 15. Comparison of the calculated ECD spectra of (*S*)-**2** and the experimental ECD spectra of (+)- and (−)-**2**.

cal activities have recently been reported for the sesquiterpene quadrone,[8] the schizozygane alkaloid schizozygine,[9] and the iridoids plumericin and isoplumericin.[10]

Methods

Oxadiazol-3-one, **2**, was synthesized as previously reported.[1]

Analytical liquid chromatography was performed on a chromatograph equipped with a 20 μL loop injector, and a chiro-optical UV/CD detector. Chromatographic data were collected and processed with Jasco Borwin software.

Semipreparative liquid chromatography was performed on a chromatograph equipped with a 500 μL loop injector, a UV SpectroMonitor 4100 spectrophotometer, and a refractive index detector.

The enantiomers of **2** were resolved by semipreparative HPLC, using a Regis Chemical Company (*R*,*R*)-DACH-DNB column (250 mm × 10 mm i.d.), *n*-hexane/dichloromethane 70/30 as eluent (flow rate 6.0 mL/min and T = 25 °C) and UV detection at 270 nm. The sample of (±)-**2** was dissolved in the mobile phase (c = 55 mg/mL); each injection was 50 μL (process yield 65%).

The enantiomeric excess, the UV, and ECD at 270 nm were determined by analytical HPLC with use of a Regis (*R*,*R*)-DACH-DNB column (250 mm × 4.6 mm i.d.) under the same conditions employed for semipreparative HPLC, excepting the flow rate (1.0 mL/min). The ECD and UV spectra of CH_3CN solutions of chromatographically resolved (+)-**2** and (−)-**2** ($c = 4.1 \times 10^{-5}$ M) were recorded with a Jasco J710 UV CD spectrometer.

IR and VCD spectra of $CDCl_3$ solutions of (+)-**2**, (−)-**2**, and (±)-**2** were measured with Thermo Nicolet Nexus 670 and Bomem/BioTools Chiral IR spectrometers, respectively. A 597 μm cell with KBr windows was used. IR and VCD spectra were measured at resolutions of 1 and 4 cm^{-1}, respectively. VCD scan times were 1 h.

Specific rotations of $CDCl_3$ solutions of (+)-**2** and (−)-**2** were measured with a polarimeter at 25 °C.

Conformational analysis of **2** was carried out initially with the MMFF94 molecular mechanics force field via the SPARTAN 02 program.[12] Conformations obtained were reoptimized with DFT via the GAUSSIAN 03 program.[4] Subsequently, potential energy surface (PES) scans were carried out with DFT to search for additional conformations, not located using MMFF94. Harmonic vibrational frequencies were then calculated for all conformations to verify their stability and to permit calculation of their relative free energies. Harmonic dipole and rotational strengths were simultaneously calculated, and IR and VCD spectra obtained thence by using Lorentzian bandshapes.[13]

Electronic excitation energies, oscillator strengths, rotational strengths, and transparent spectral region specific rotations of **2** were calculated using TDDFT via the GAUSSIAN 03 program. Electronic rotational strengths were calculated using both length and velocity representations. ECD spectra were obtained from electronic excitation energies and velocity rotational strengths using Gaussian bandshapes.[6c]

Acknowledgment. We are grateful for financial support from the National Science Foundation (to P.J.S., Grants CHE-0209957 and CHE-0614577) and for computer time at the USC High Performance Computing and Communication (HPCC) facility and at Hewlett-Packard Inc.

Supporting Information Available: Calculated dihedral angles, calculated and experimental frequencies, dipole strengths and rotational strengths, and calculated electronic excitation energies, oscillator strengths, and rotational strengths of **2**; calculated IR and VCD spectra of conformations **a**−**c** of **2**; comparison of calculated and experimental vibrational frequencies of **2**; optimized geometries of conformations **a**−**c** of **2**. This material is available free of charge via the Internet at http://pubs.acs.org.

JO070302K

(15) Andreani, A.; Billi, R.; Cosimelli, B.; Mugnoli, A.; Rambaldi, M.; Spinelli, D. *J. Chem. Soc., Perkin Trans. 2* **1997**, *11*, 2407−2410.